Industrial Crops & Products 222 (2024) 119734

Contents lists available at ScienceDirect

Industrial Crops & Products

journal homepage: www.elsevier.com/locate/indcrop

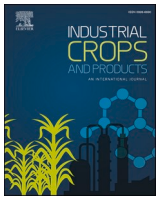

Vegetable oil-derived polyether-polyester thermosets: Solvent-free synthesis and mechanical properties

Esperanza Cortés-Triviño [a,*], Susana Fernández-Prieto [b], Inmaculada Martínez [a], José M. Franco [a]

[a] Pro2TecS-Chemical Product and Process Technology Centre, University of Huelva, Huelva 21071, Spain
[b] Procter and Gamble Brussels Innovation Center, Strombeek-Bever 1853, Belgium

ARTICLE INFO

Keywords:
Sustainable polymeric thermosets
Solvent-free synthesis route
Epoxy resins
Curing kinetics
Rheological properties

ABSTRACT

Vegetable oils differing in the number and kind of reactive chemical sites were investigated as potential feedstock in reactions involving epoxy rings to produce sustainable polymeric thermosets. Sustainable polyether-polyester matrices were synthesized through the mixing of three different vegetable oils (castor, tung and sunflower oil) with maleic anhydride to promote their chemical activation, and subsequently induce the reaction with polyethylene glycol diglycidyl ether (PEGDGE). The interactions between double bonds and/or hydroxyl groups present in vegetable oils, anhydrides and epoxy rings within a solvent-free medium promote the expected chemical crosslinking, yielding polymeric thermosets that encompass the Green Chemistry tenets. Fourier transform infrared spectroscopy, thermogravimetric analysis, and differential scanning calorimetry tests were employed to validate the chemical reactions taken place during the synthesis, as well as to monitor the kinetics of curing. Moreover, a rheological characterization was conducted to assess the influence of both the vegetable oil and the ratio of reactive components on the ultimate mechanical properties. Although chemical crosslinking was suitably attained in all the systems studied, a more reinforced network with values of the storage modulus (G') of $54{\cdot}10^5$ Pa was obtained in those based on tung oil possessing the higher quantity of reactive functional sites; meanwhile, the presence of hydroxyl groups within the vegetable oil structure led to the production of more flexible thermosets (G' of $6.2{\cdot}10^5$ Pa).

1. Introduction

Polymeric thermosets encompass a group of polymers that, upon curing, undergo a chemical cross-linking reaction leading to the formation of a permanent rigid three-dimensional network structure. Included in this category, polyurethanes are the most predominant ones commercially available, which may cover a wide range of applications including foams, coatings, or adhesives, among others (Brzeska and Piotrowska-Kirschling, 2021; Echeverria-Altuna et al., 2022). Nevertheless, their production relies on petroleum-based raw materials and involves the use of potentially harmful compounds like isocyanates, which prompts researchers to seek more sustainable alternatives while preserving their fundamental properties. Exploring potential replacements for polyurethanes, epoxy resins offer intriguing possibilities as thermosetting materials, which can be used in many industrial applications like electronic insulation devices, encapsulation or transportation and construction materials due to their outstanding fundamental properties (Kotb et al., 2022; Liu et al., 2022). They are formed through a chemical reaction between an epoxy monomer and a curing agent or hardener, resulting in the creation of a robust crosslinked network. To date, the majority of commercially available epoxy resins are synthesized using precursors derived from bisphenol A, and amines as curing agents, which are recognized to represent health concerns due to their toxicological properties (Devansh et al., 2024; Morsch et al., 2023; Rosu et al., 2015). Consequently, ongoing efforts are being undertaken to address both the environmental and human health challenges by exploring and developing sustainable and eco-friendly options for traditional epoxy resins. A feasible approach to substitute these compounds that has emerging strongly in recent years deals with the development of epoxy-based thermosets with green characteristics and/or derived from renewable resources. However, although ongoing research is being conducted to address this challenge, the achievement of fully sustainable thermosetting formulations still requires substantial advancement. This is because the majority of these materials continue to

* Correspondence to: Departamento de Ingeniería Química. Campus de "El Carmen", Universidad de Huelva, Huelva 21071, Spain.
E-mail address: esperanza.cortes@diq.uhu.es (E. Cortés-Triviño).

https://doi.org/10.1016/j.indcrop.2024.119734
Received 3 July 2024; Received in revised form 27 August 2024; Accepted 21 September 2024
Available online 26 September 2024

use solvents or reagents that do not entirely align with the Principles of Green Chemistry (Hasan and Bircan, 2022; Nabipour et al., 2023; Zhen et al., 2024). For instance, Zhen et al. studied the development of bio-based epoxy resins from epoxidized vegetable oils and lignin using *N,N*-dimethylformamide and 4-dimethylaminopyridine as solvents (Zhen et al., 2024). Likewise, Nabipour et al. also obtained bio-based epoxy resins with excellent mechanical properties but employing some harmful reagents like epichlorohydrin, ethanol or dichloromethane, among others (Nabipour et al., 2023). Aiming to overcome these drawbacks regarding the use of detrimental chemicals, the achievement of sustainable polymeric thermosets from bio-based resources, following a solvent-free synthesis route and avoiding the use of reagents with adverse environmental implications, is explored in this investigation. Thus, polyethylene glycol diglycidyl ether (PEGDGE) offers several benefits as a non-toxic epoxy monomer commercially available, which can act as a crosslinking agent in the production of epoxy resins. By possessing a long-chain structure with two epoxy groups at its ends, this epoxide fosters the formation of a strong three-dimensional network when it interacts with curing agents such as amines or acid anhydrides, offering the final epoxy formulations superior chemical resistance, formidable adhesion, and/or heightened mechanical strength (Amirova et al., 2016; Balgude et al., 2017; Kubota et al., 2024). Therefore, the reaction of PEGDGE with anhydrides, like maleic anhydride, may represent an interesting option to explore the sustainable production of epoxy-based thermosets. As well-known, maleic anhydride is a common reagent employed in a wide variety of industrial processes due to its great versatility in producing different intermediate compounds for multiple applications (Chen et al., 2023; Delli et al., 2024; Felthouse et al., 2000). Although it is not typically considered as a totally "green" substance, maleic anhydride can be synthesized from renewable resources, also contributing to minimizing the environmental impact in solvent-free processes (Cucciniello et al., 2023). However, some researchers have demonstrated that anhydrides do not directly react with epoxy groups. Instead, they require first the opening of anhydride rings through initiation reactions with other suitable reactive compounds leading to the formation of a monoester containing a carboxylic acid group, which subsequently becomes available for further interaction with epoxides (Kolář and Svítilová, 2007). Hence, the curing reactions involved in the synthesis of epoxy resins chemically modified with anhydrides encompass different chemical interactions comprising initiators, catalysts and/or high temperatures (Fombuena et al., 2019; Wu et al., 2024). Indeed, a majority of researchers have reported the use of tertiary amine catalysts to facilitate the reaction of an epoxy-anhydride system, giving rise to a crosslinked network and the formation of polymeric thermosets. However, notable environmental concerns arise due to the detrimental characteristics of amines, even when employed solely as catalysts (Huang et al., 2015).

In this respect, vegetable oils, recognized as renewable and sustainable raw materials per excellence, contain both unsaturation and/or hydroxyl groups within their chemical composition, thus making them excellent precursors to chemically activate anhydrides (Eren et al., 2003; Kale et al., 2019). For instance, tung oil, sunflower oil or castor oil, offer distinctive properties that make them valuable for the synthesis of novel polymeric materials particularly when activated with anhydrides. Among them, the above-mentioned unsaturation degree or the presence of hydroxyl groups within their chemical structures, their inherent chemical and water resistance, or their plastizing properties, contribute to their effectiveness in this context. Additionally, their renewable and biodegradable character and their reactivity, for instance with anhydrides, further reinforce their potential as excellent candidates for creating a wide range of new sustainable materials (Sharma and Kundu, 2006). In this sense, the chemical reaction with anhydrides yields maleated vegetable oils, thereby significantly enhancing the sustainability aspect of the synthesized polymeric thermosets by increasing their renewable character. There are several mechanisms by which anhydrides can chemically modify vegetable oils. For instance, these modifications can occur via Diels-Alder reactions in oils containing conjugated dienes, through esterification in oils comprising hydroxyl groups, and/or using 'ene-reactions' in oils containing allylic hydrogens (Dayanne et al., 2018). For unsaturated vegetable oils, many authors suggested the formation of a new carbon-carbon bond between the fatty acid and the anhydride ring, with the subsequent shifting of the allylic hydrogen and the loss of the double bond of maleic anhydride. In those cases, the substitution takes place in the carbon double bonds of the vegetable oil molecule (Amos et al., 2021). However, when using a vegetable oil comprising hydroxyl groups in its chemical structure, like castor oil, the interaction with maleic anhydride involves the substitution of the hydroxyl groups of castor oil by the maleic anhydride. This is due to the higher susceptibility to substitution of this group by other chemical compounds in comparison with their double bond's counterparts (Dayanne et al., 2018). In both cases, these maleated vegetable oils comprise a carboxylic group of monoester which would be prone to react with the epoxy groups contained in glycidyl ether compounds in the presence of accelerators, generating a diester and a new hydroxyl group via nucleophilic attack with the subsequent epoxy ring opening (Amirova et al., 2016; Fombuena et al., 2019).

These chemical reactions taking place between these three raw materials would generate chemical crosslinked networks with suitable properties to be applied in different fields. This study focuses on the preparation of polymeric thermosets based on PEGDGE, maleic anhydride and vegetable oils (i.e., polyester- and polyether-based matrices) following a relatively simple and solvent-free synthesis route. The resulting materials exhibit promising mechanical properties that allow them to be proposed as sustainable alternatives to polyurethanes. In this sense, careful consideration has been given to accomplishing the Green Chemistry principles in the synthesis of polymeric thermosets. Special emphasis has been placed on selecting less hazardous chemical synthesis methods to minimize the environmental impact, also preventing waste production, and optimizing the atom economy by promoting the use of renewable materials. Additionally, the design of safer products, the use of solvent-free processes and the incorporation of renewable and/or eco-friendly resources have been prioritized, as well as the incorporation of catalyst compounds to improve efficiency and minimize the need for excess reagents (Anastas and Eghbali, 2010). Through all these efforts, this study seeks to promote sustainability and reduce the ecological footprint of the chemical processes involved, positioning these polymeric materials as promising alternatives to traditional non-sustainable polyurethanes and polyesters. The influence of the type of vegetable oil, reflected in the number and kind of functional sites susceptible to chemical modifications, on the rheological properties of the final epoxy-based thermosets, as well as the kinetics and reaction pathways taking place during the curing process, have been explored in this work.

2. Experimental section

2.1. Materials

Castor oil (CO, Guinama, Valencia, Spain), tung oil (TO, Merck-Sigma Aldrich, St. Louis, USA) and sunflower oil (SO, local supermarket, Spain) were selected as vegetable oils to synthesize the sustainable polymers via crosslinking reaction with maleic anhydride (puriss., ≥99 %), and polyethilene glycol diglycidyl ether (PEGDGE, average M_n: 500 g/mol), both supplied by Merck-Sigma Aldrich (St. Louis, USA). Tetra-n-butylammonium bromide (TBAB, ≥98 %) was employed as a reaction accelerator.

2.2. Synthesis of polymeric thermosets

Epoxy-based polymeric thermosets were synthesized by mixing the vegetable oil and the epoxy compound in an open vessel until 100 °C was reached. Then, the desired amount of maleic anhydride was added to the mixture, increasing the temperature to 110 °C. When the

temperature was established, 1 wt% of catalyst (over total weight) was incorporated, and the reaction was carried out for 25 min to get a homogeneous solution. After cooling down the mixture by immersing the vessel in an ice-containing bath, 12 g of sample was poured into rectangle silicon moulds (dimensions: 8 ×5.5 ×2.5 cm in length, width, and thickness, respectively), which were placed in an oven and heated at 120 °C for 20 h to accomplish the curing process (see Fig. 1). The reagent proportions and sample codes are shown in Table 1, meanwhile, Fig. 2 shows the reaction mechanisms occurring during the synthesis, considering that sunflower oil follows the analogous reaction of tung oil.

Table 1
Composition of the synthesized polymeric thermosets (CO, TO and SO in sample code refer to castor, tung and sunflower oils, respectively).

Samples code	Oil (%)	Maleic Anhydride (%)	Epoxy compound (%)	C═C*/Anhydride/ Epoxy molar ratios
CO−1–1–1	47.06	14.83	37.81	1/1/1
TO−1–1–1	21.64	21.95	55.96	1/1/1
SO−1–1–1	33.36	18.67	47.59	1/1/1
CO−0.5–1–1	30.80	19.41	49.49	0.5/1/1
CO−1.5–1–1	57.13	11.99	30.57	1.5/1/1

2.3. Characterization techniques

Fourier transform infrared (FTIR) spectra of final or incipient (i.e. during curing) thermosets based on castor, sunflower and tung oil, as well as the raw materials such as neat oils, maleic anhydride and PEGDGE were acquired using an FT/IR-4200 spectrometer (JASCO, Tokyo, Japan) coupled with an attenuated total reflectance (ATR) accessory containing a monolithic diamond crystal. FTIR spectra were recorded in transmission mode at a resolution of 4 cm^{-1} in the wavenumber range of 400–4000 cm^{-1}.

A Q-50 thermal analyser (TA Instruments Water, USA) was used to assess the thermal degradation patterns of the raw materials and the synthesized formulations. Samples (10–20 mg) were placed in platinum pans, and mass losses were quantified by applying a temperature ramp from 30 °C to 600 °C at 10 °C min^{-1} under a nitrogen atmosphere.

Differential scanning calorimetry was analyzed by using a DSC250 (TA Instruments, New Castle, USA). ~10 mg of fully-cured or incipient (i.e. during curing) thermosets were placed in sealed aluminium pans and inserted in the measurement heating cell. Samples were heated while applying a nitrogen flow of 50 ml min^{-1} from −80–200 °C at 10 °C/min.

Rheological characterization of fully-cured thermosets was performed using an ARES G2 rheometer (TA Instruments, USA) equipped with torsion geometries. Small-amplitude oscillatory torsional tests in the linear viscoelastic regime were performed in a frequency range of 0.03–100 rad/s at 25 °C. Prior to the tests, rectangular specimens of dimensions of 35±2, 12.8±0.3 and 2.38±0.3 mm in length, width, and thickness, respectively, were obtained with the aid of a die cutting machine (ATS Faar, S.p.A, Milano, Italy).

At least two replicates of each experimental measurement or analysis were performed on fresh samples.

3. Results and discussion

3.1. FTIR

The chemical reaction occurring between the three different raw materials promoted by the catalyst action of the ammonium quaternary salt was deeply studied through infrared spectroscopy. Fig. 3 shows the FTIR curves for the new synthesized products based on the three types of oils in comparison with the pure raw materials. Thus, the different oils showed similar vibration peaks relative to their closely related molecular structure, with the exception of the peak corresponding to the hydroxyl groups (O−H stretching vibrations) in the castor oil spectrum, which was shown at around 3400 cm^{-1} (Panhwar et al., 2019). Apart from that, all of them displayed some common vibration bands like the relative to the C−H stretching vibrations of the cis-double bond at 3007 cm^{-1}, or others located between 2980 and 2800 cm^{-1} typical of asymmetrical and symmetrical stretching vibration of aliphatic $-CH_3$, $-CH_2$ fatty acid hydrocarbon chain. Moreover, the characteristic stretching band of triglyceride (C═O functional group) was detected at 1742 cm^{-1}, together with cis C═C stretching vibration at 1642 cm^{-1}, bending vibrations of $-CH_2$ scissoring aliphatic groups at 1460 cm^{-1}, and bending vibrations of $-CH_2$ at 1375 cm^{-1} (Rohman and Che Man, 2012). The ester carbonyl group (C−O−C) typical of vegetable oils was detected due to its bending vibrations at 1238, 1156, 1097 and 1030 cm^{-1}. Finally, the peaks displayed at around 990–970 cm^{-1}, which were more remarkable in tung oil spectrum (Schönemann and Edwards, 2011), were assigned to the vibrations of HC═CH (trans) bending out of plane, while at 860 cm^{-1} and 722 cm^{-1}, the $=CH_2$ wagging vibrations and $-CH_2$ rocking out of plane vibration of long chain fatty acid, respectively, took place (Fahmi et al., 2020; Silva et al., 2021; Yi et al., 2019; Zhang et al., 2020).

However, when modifying the three types of oils with maleic anhydride and PEGDGE to obtain crosslinked materials, several differences in the spectra were detected as a result of the different chemical reactions. As mentioned above, vegetable oils are expected to react with maleic anhydride via C═C scission (Xiao et al., 2020) or castor oil hydroxyl groups interaction (Alves et al., 2022), obtaining maleated vegetable oils capable of successfully reacting with epoxy compounds. In this sense, as can be noticed from Fig. 3a noticeable decrease in the intensity of the band at 3007 cm-^{1}, relative to the C−H stretching vibration of the cis double bond of fatty acids, was detected for the three types of oil, which confirm the reaction with maleic anhydride via double bond scission. This was further corroborated in the case of tung oil, whose spectrum revealed the complete disappearance of HC═CH (trans) bending out of plane vibration bands at around 990–970 cm^{-1}. Regarding castor oil, a noticeable variation in the intensity of the vibration band related to the O−H bond at 3400 cm^{-1} must be highlighted, which suggests that the chemical modification also took place through the cleavage of its hydroxyl groups (Şahin et al., 2016). Moreover, the binding of maleic anhydride into the oil molecular structure

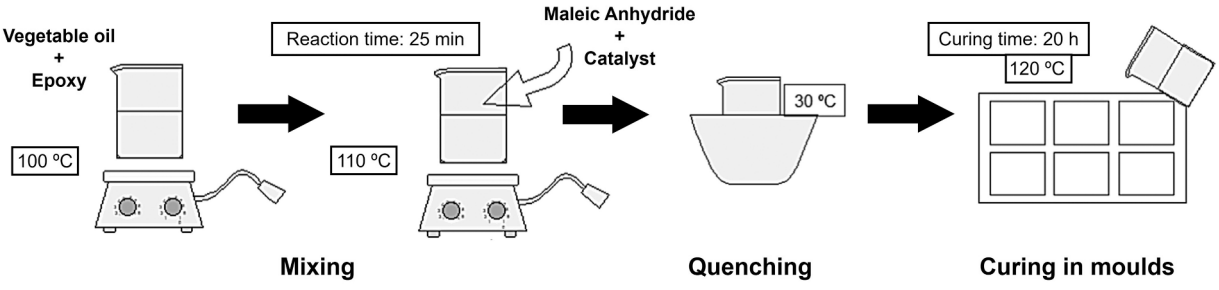

Fig. 1. Schematic flow diagram of the process followed to synthesize the polymeric thermosets.

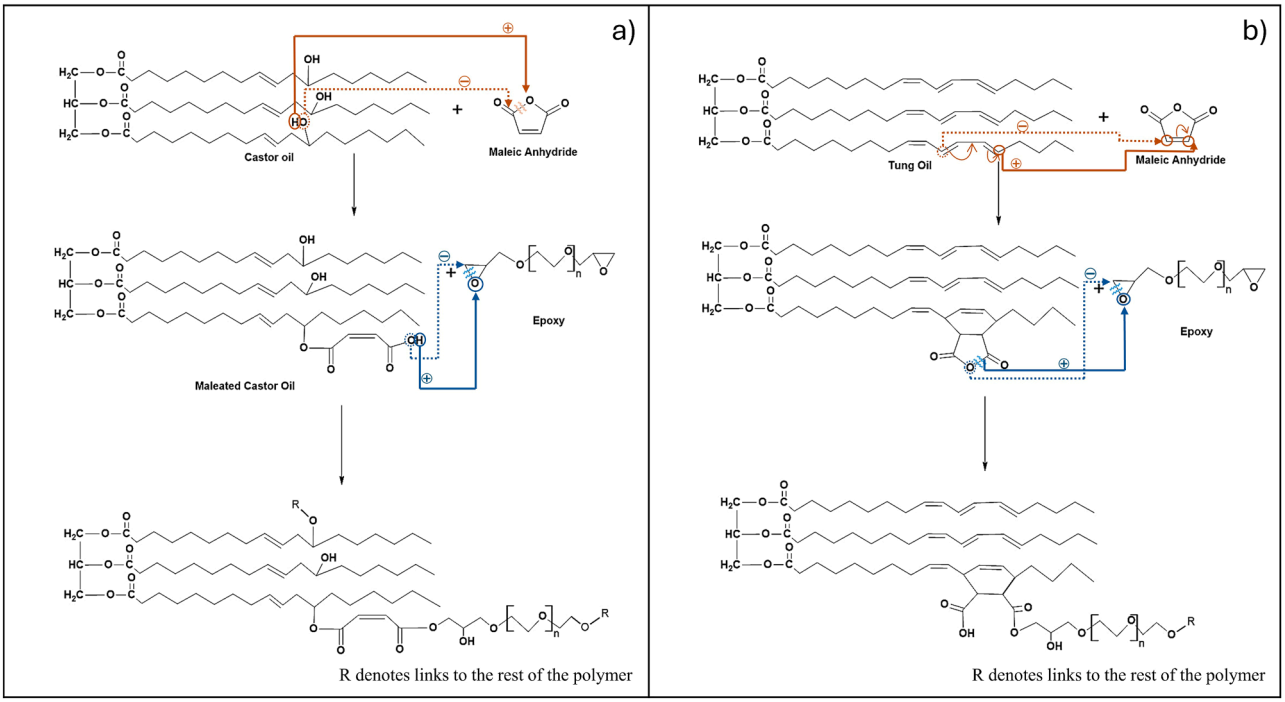

Fig. 2. Scheme of the chemical reactions involved in the synthesis of a) castor oil-based and b) tung oil-based polymeric thermosets. More detailed mechanistic insights of these reactions can be found elsewhere (Thakur et al., 2018; Tran et al., 2005).

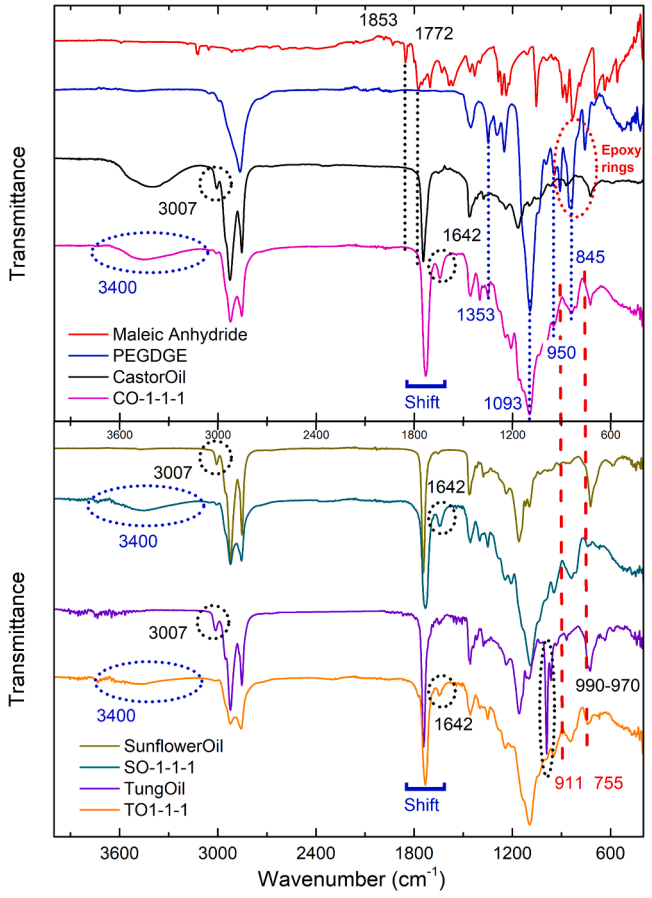

Fig. 3. FTIR spectra for synthesized polymeric thermosets in comparison with neat raw materials.

could be verified through the increase in the peak at 1642 cm^{-1} because of the formation of new C═C linkages after its reaction with both nonconjugated double bonds and/or hydroxyl groups (Poletto, 2019; Tran et al., 2005; Wazarkar and Sabnis, 2018). On the other hand, the consumption of the total amount of maleic anhydride during the reaction could be corroborated by the absence of cyclic anhydride absorption bands observed at 1853 and 1772 cm^{-1} in the new synthesized materials spectra (Alves et al., 2022).

On the other hand, the chemical crosslinking produced when reacting the maleated vegetable oils with the epoxy compound (PEGDGE) can also be corroborated by FTIR analysis. The nucleophilic attack of epoxy rings with maleic anhydride moieties through −COOH chemical sites is expected to occur, generating new hydroxyl groups as a consequence of the oxirane rings opening (Amirova et al., 2016), as can be seen in Fig. 2. This fact can be deduced from the spectra of Fig. 3, where a new and slight band at around 3400 cm^{-1} was identified for SO and TO-based polymeric thermosets. In the case of samples synthesized with CO, the hydroxyl groups forming its molecular structure are expected to fully react with maleic anhydride, thus disappearing this vibration band at the end of this chemical reaction and re-emerging after epoxy grafting (Saeedi et al., 2019). Moreover, the binding of maleic anhydride to vegetable oil triglycerides and its further reaction with epoxy rings can be also verified using the C═O ester group vibration band, which was shifted from 1742 to 1720 cm^{-1} in the spectra of all new synthetized materials (Khundamri et al., 2019; Wazarkar and Sabnis, 2018). On the other hand, the existence of new peaks in the spectra of polymeric thermosets, at 1093 and 950 cm^{-1}, relative to C−O−C stretching vibration, and those associated with C−H bending vibration bands at 1353 and 845 cm^{-1} from the PEGDGE structure, would confirm the incorporation of the epoxy network into the molecular structure (Teng et al., 2017). Finally, the vibration bands related to oxirane at 911, 856 and 755 cm^{-1} (C−O and C−O−C stretching of the epoxy group) shown in the molecular structure of PEGDGE, were not visible in the three synthesized biopolymers curves, thus confirming the completion of the crosslinking reactions due to the non-existence of closed epoxy rings (Khundamri et al., 2019; Tudorachi and Mustata, 2020; Yang et al., 2016).

To better understand the curing process of samples, FTIR of castor oil-based formulation was monitored for 20 h and selected spectra are shown in Fig. 4. As detailed above, raw materials were mixed in different steps, first adding the vegetable oil and PEGDGE and heating up to 100 °C, then incorporating maleic anhydride and increasing temperature to 120 °C, and finally adding the catalyst. In this sense, the first spectrum shown in Fig. 4(t-15 min) was taken 15 min after the addition of all reagents, when the mixture acquired a certain viscosity (60 cP approx.). At this point, the crosslinking reaction seems to be progressing, not only by detecting an increase in the viscosity of the mixture but also by a reduction in the vibration bands related to O−H and C−H of the cis double bonds at 3400 and 3007 cm^{-1}, respectively, as well as the appearance of a new band at 1642 cm^{-1} associated with the formation of new C═C linkages after the opening of the anhydride ring and the further reaction with double bonds and/or hydroxyl groups. However, the presence of some vibration peaks at 1853 and 1772 cm^{-1} related to the cyclic anhydride reveals that there are still moieties of unreacted maleic anhydride in the mixture. In addition, the bands at around 950–750 cm^{-1}, also confirmed the existence of the oxirane group in the mixture.

Following the defined protocol, after 25 min of mixing, the blend was cooled down, poured into silicon moulds, and placed in an oven at 120 °C for curing (t0h curve, referred to the moment the sample was placed in the oven). At this moment, the total consumption of remaining maleic anhydride moieties was verified, as its characteristic bands on the FTIR spectrum disappeared (1853 and 1772 cm^{-1}). Nevertheless, as deduced from the small vibration signals shown at 911, and 755 cm^{-1}, oxirane rings were still present in the polymer network when the moulds were placed in the oven, thus still having a non-fully crosslinked material with a predominantly viscous consistency. The progress of the crosslinking reaction can be monitored by calculating the peak area related to epoxy rings (911 cm^{-1}) as a function of time and correlating this with a reference vibration band which remains constant during the chemical reaction, for instance, that corresponding to C═O of triglyceride (1730 cm^{-1}). The evolution of such a ratio between the areas related to both the epoxy ring vibration peak (A_{epoxy}) and the reference and non-variable C═O signal ($A_{C=O}$) is shown in Fig. 5a as a function of curing time. As can be seen, after approximately 5–6 h, no significant variation in this ratio is produced and therefore the curing process can be considered virtually completed.

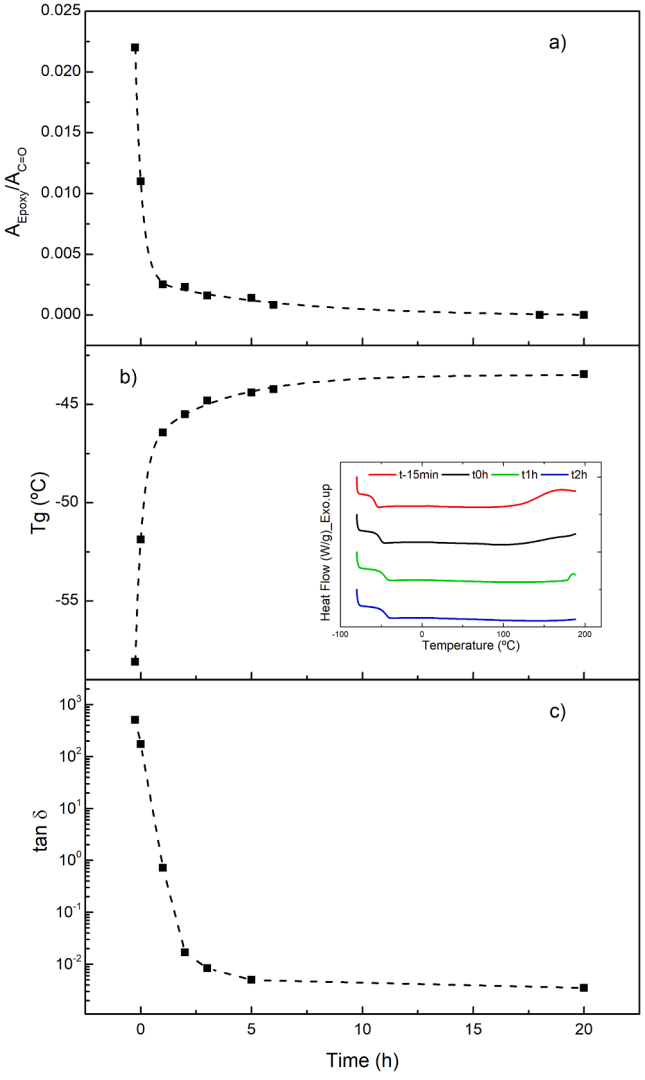

Fig. 5. Kinetic evaluation of the curing reaction for castor oil-based polymeric thermosets (sample CO-1–1–1) by means of a) epoxy ring evolution in FTIR, b) glass transition temperature in DSC, and c) tan δ in rheological tests.

3.2. TGA

A thermogravimetric analysis of the synthesized polymeric thermosets was also performed to verify the chemical crosslinking occurring

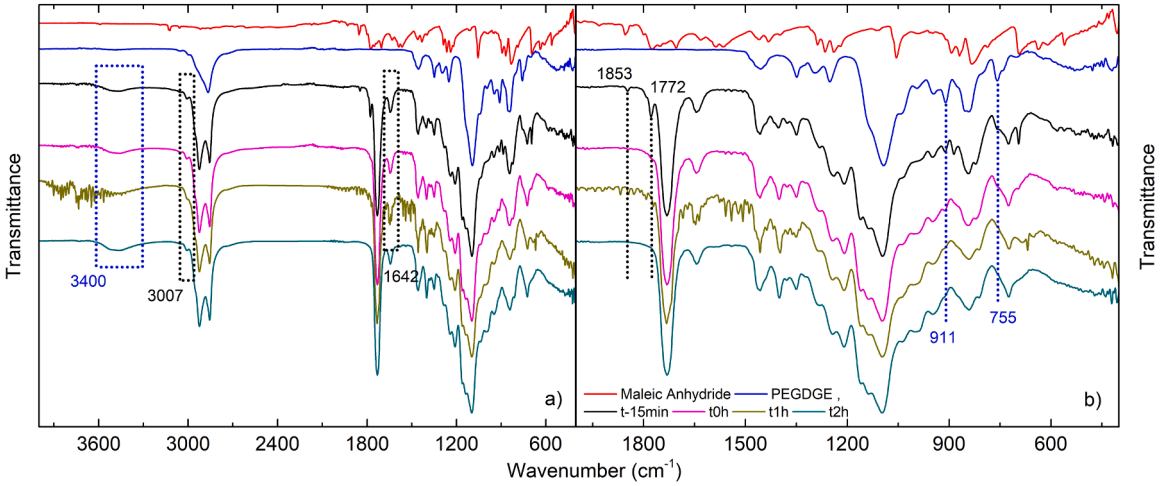

Fig. 4. Monitoring the curing process by FTIR as a function of time for castor oil-based prototypes.

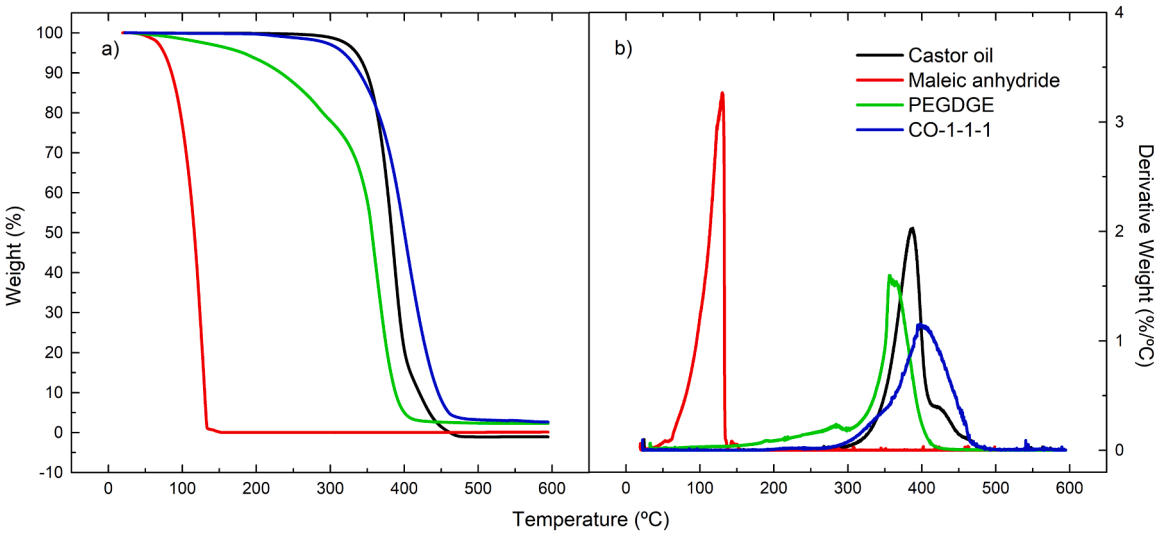

Fig. 6. Loss weight (a) and decomposition-rates (b) curves during the thermal degradation for raw materials and the castor oil-based thermoset.

Table 2
Thermogravimetric typical parameters for the three synthesized polymers thermosets and their corresponding raw materials.

Sample	T_{onset} (°C)	T_{max} (°C)	T_{final} (°C)	ΔW(%)	Residue (%)
Castor oil	359	388	410	100	0
Sunflower oil	381	421	437	99.9	0.1
Tung Oil	390	425	455	99.4	0.6
Maleic Anhydride	88	130	133	99.9	0.1
PEGDGE	217/344	284/356	291/391	21.8/75.9	2.3
CO−1–1–1	357	398	443	97.3	2.7
SO−1–1–1	350	383	425	94.6	5.4
TO−1–1–1	356	376	429	93.9	6.1

between the different components. Regarding the starting materials, as can be deduced from the curves and data shown in Fig. 6 and Table 2, all vegetable oils showed the most important degradation peak at around 380–425 °C (referred to as the maximum degradation rate, T_{max}), which is mainly related to thermal decomposition of unsaturated fatty acids of oils (Gomna et al., 2020; Gouveia De Souza et al., 2004). In this sense, some differences between oils are identified in terms of their temperature resistance. Since tung oil is mainly composed of triglycerides of α-eleostearic acids, oleic acid, and linoleic acid, its molecular structure comprises the highest number of unsaturations compared to castor and sunflower oils (Schönemann and Edwards, 2011), thus showing the highest T_{max}, i.e. 425 °C. As some authors pointed out, the existence of glyceryl esters of saturated fatty acid chains tends to degrade thermally faster than unsaturated chain fats, therefore shifting this peak to higher temperatures as the number of C═C in the oil microstructure increases (Subramanian, 2019; Tang et al., 2020). Moreover, all types of oils showed a small shoulder in their decomposition curves at around 450–500 °C, responsible for the decomposition of secondary components present in the oil, including the formation of by-products.

Concerning the decomposition profile of the synthesized polymeric thermosets, these showed a single thermal degradation event at T_{max} of around 379–400 °C, which is in accordance with the thermal degradation temperature reported for similar bio-based epoxy-based crosslinked polymers (Mattar et al., 2020; Şahin et al., 2016). The absence of degradation peaks at lower temperatures confirms the total consumption of unreacted raw materials during the synthesis process, i.e. both maleic anhydride and PEGDGE, whose T_{max} are found at 130 and 284 °C, respectively, as a consequence of the chemical crosslinking previously described (Omonov et al., 2019; Parada Hernandez et al., 2019). However, a slight decrease in the decomposition temperatures (both in T_{onset} and T_{max}) of SO-1–1–1 and TO-1–1–1 materials was noticed in comparison to their oil counterparts. This can be explained by the increase in the number of ester groups forming the microstructural network after the chemical crosslinking, leading to a slight reduction in the thermal stability of the resulting polymeric materials (Liu et al., 2015). Instead, for the castor oil-based formulations, the thermal degradation profile remains almost similar to that shown by the pure oil, which could be justified by the new C═C functionalities produced during the crosslinking process, which enhances the thermal resistance, apart from the negative contribution of the new formed ester groups (Tang et al., 2020). Finally, as can be seen in Fig. 6, the slower degradation rate at high temperature of the CO-1–1–1 sample (see the shoulder of the peak in the derivative curve) also verifies the crosslinking reactions occurring via epoxy ring scission with maleated groups.

3.3. DSC

Fig. 7, 8 shows the differential scanning calorimetry curves of polyether-polyester thermosets in comparison to their raw materials counterparts. In agreement with the existing literature, castor oil shows a regular glass transition at −64 °C (Tamási and Marossy, 2022), meanwhile, other complex thermal events were displayed by sunflower and tung oil. The first one exhibited two small exothermic peaks in the cooling ramp at −16 °C and −50 °C corresponding to the both phase transition of saturated fatty acid chains and low-melting unsaturated oil fraction, respectively. During the heating, the first melting of a crystallized portion of sunflower oil takes place at −69 °C, followed by a re-crystallization and re-organization of polymorphic structures prior to the progressive melting of all crystals at −20 °C (Calligaris et al., 2008). A similar trend was shown by tung oil, which exhibited similar exothermic events due to the saturated and unsaturated portions at −36 and −48 °C, respectively, in the cooling ramp. Likewise, during the heating, the first melting followed by a re-crystallization was detected at −69 °C, in this case reaching the progressive melting slightly earlier at −33 °C. Regarding the derived bio-based polyether-polyesters, these formulations did not show any of these thermal events in the DSC curves, which indicates there are no free double bonds in the oil structure, as well as no anhydride or epoxy groups in the polymer after accomplishing the curing process (see Fig. 6). In this sense, the non-existence of peaks at around 50 °C confirms the total reaction of maleic anhydride moieties (Johns et al., 2016; Sain et al., 2020). Also, the total consumption of free epoxy rings in the polymer molecular structure was confirmed by the

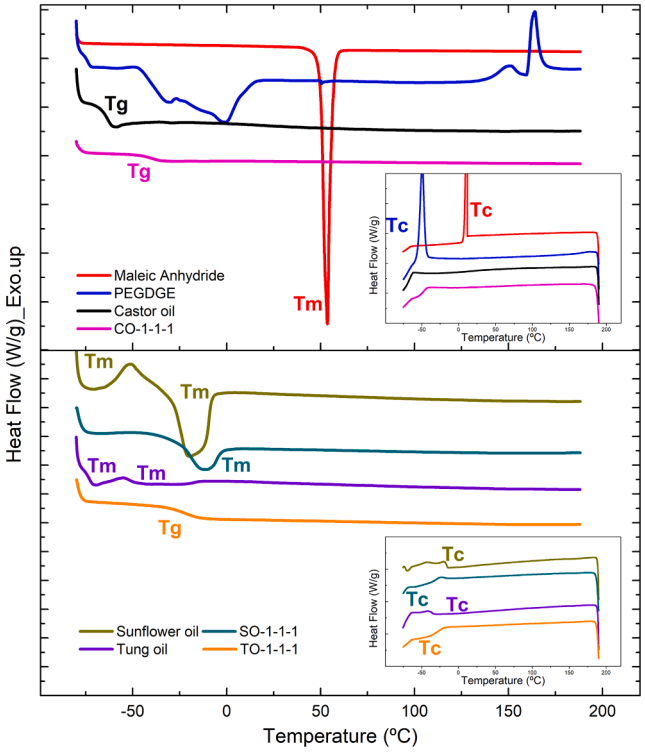

Fig. 7. Differential scanning calorimetry curves for the synthesized thermosets. Heating ramps from 200 to −80 °C and cooling ramps in the insets.

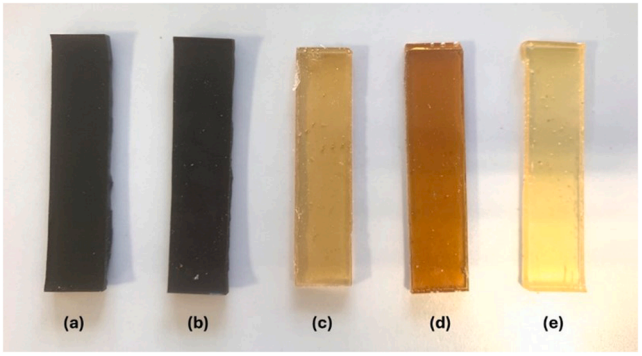

Fig. 8. Visual appearance of polymeric thermosets: a) TO-1–1–1, b) SO-1–1–1, c) CO-1–1–1, d) CO-0.5–1–1, and e) CO-1.5–1–1.

disappearance of the exotherms related to epoxy groups at around 150–200 °C (Jourdain et al., 2020). The fully cured polymeric thermosets just showed regular glass transitions for castor and tung oil-derived materials, and a melting event in the case of the sunflower oil-derived polyether-polyester (see Table 3), at higher temperatures than their corresponding base oils, which indicates an enhancement in the intermolecular forces of the chemical structure due to hydrogen bonding eventually leading to chain mobility hindrance (Balgude et al., 2017; Michel and Ferrier, 2020).

Table 3
Thermal events occurring in polymeric thermosets in comparison with the neat raw materials.

Sample	T_g/T_m (°C)	T_m (°C)
Castor oil	−64	
Sunflower oil		−69; −20
Tung Oil		−69; −33
CO−1–1–1	−40.2	
SO−1–1–1	−12.5	
TO−1–1–1	−22.4	
CO−0.5–1–1	−31.8	
CO−1.5–1–1	−38.6	

The curing process can also be monitored by DSC analyzing the evolution of the glass transition temperature, T_g, as a function of the curing time, as shown in Fig. 5b for one selected formulation (CO-1–1–1). The glass transition was gradually shifted towards higher temperatures as curing time progressed, confirming the chemical crosslinking (Balgude et al., 2017) and, as can be seen, an almost constant T_g value was reached after 5–6 h, upon completion of the curing process, in agreement with the data obtained from FTIR analysis.

3.4. Rheology

After chemical crosslinking, solid-like formulations with similar consistency and visual appearance were obtained regardless of the base oil used to synthetize the bio-based polyether-polyesters (see Fig. 7). Fig. 9 shows the evolution of the viscoelastic functions with frequency obtained in torsional mode in the linear viscoelastic regime, respectively the storage (G') and the loss (G'') moduli and the loss tangent (tan δ), for the fully cured polymeric thermosets as a function of the vegetable oil employed as raw material. In general, the three curves showed values of the elastic (G') modulus much higher than those shown by the viscous (G'') one over the whole frequency range studied, corresponding to the so-called "rubbery plateau region" of the mechanical spectrum. This viscoelastic solid-like behaviour is typically observed in fully cured materials with a well-defined crosslinked three-dimensional network (Raghavan et al., 1996). However, some differences in the viscoelastic response were detected depending on the type of oil employed to synthesize the polymers. The values of both viscoelastic parameters increased as the number of functional sites in the oil fraction rose, with the tung oil-based polyether-polyester, which included 9 double bonds, showing the highest values of both rheological moduli. This effect can be explained by the formation of a stronger network dominated by a higher number of crosslinking points arising from the double bonds of this vegetable oil. As discussed above, the chemical interaction between the double bonds of the vegetable oil and maleic anhydride generates functional sites susceptible to reacting with the oxirane rings of the PEGDGE (Eren et al., 2003; Thakur et al., 2018), thus producing a more extensively reinforced network as the number of crosslinking points increases. In addition, whilst the G' values were constant, and can be associated with the plateau modulus, G_N^0, defined elsewhere (Baumgaertel et al., 1992), G" steadily increased with frequency, indicating a close transition from the plateau to the glass transition region at this temperature. Alternatively, a reduction in the number of reactive sites dominating the vegetable oil used to synthesize the bio-based polyether-polyesters, i.e. sunflower or castor oils, with less reactive sites available for chemical modification, 5 and 3 respectively, gave rise to a notable decrease in both viscoelastic functions, showing the last one the lowest moduli due to the more flexible microstructural network obtained via reaction with hydroxyl groups. Moreover, a slight decrease in the slope of the G" curve can be also detected for these two polyether-polyesters at low frequencies, which suggests a shorter extension of the plateau region, thus highlighting the stronger gel characteristics of the tung oil-based polyether-polyester. However, the castor-oil-based polyether-polyester showed a stronger relative elastic response, i.e. lower loss tangent values (tanδ=G"/G'), with differences in G' and G" values of almost three orders of magnitude in the whole frequency range studied despite the lower values of both viscoelastic functions Fig. 9b. This aligns with the glass transition temperatures obtained from DSC tests (see Table 3), wherein the CO-1–1–1 sample exhibited the lowest value (-40 ºC) in comparison to its counterparts.

Aiming to analyze the kinetics of the crosslinking reaction, the evolution of the dynamic functions with frequency was monitored during the curing process of the polyether-polyesters, as shown for

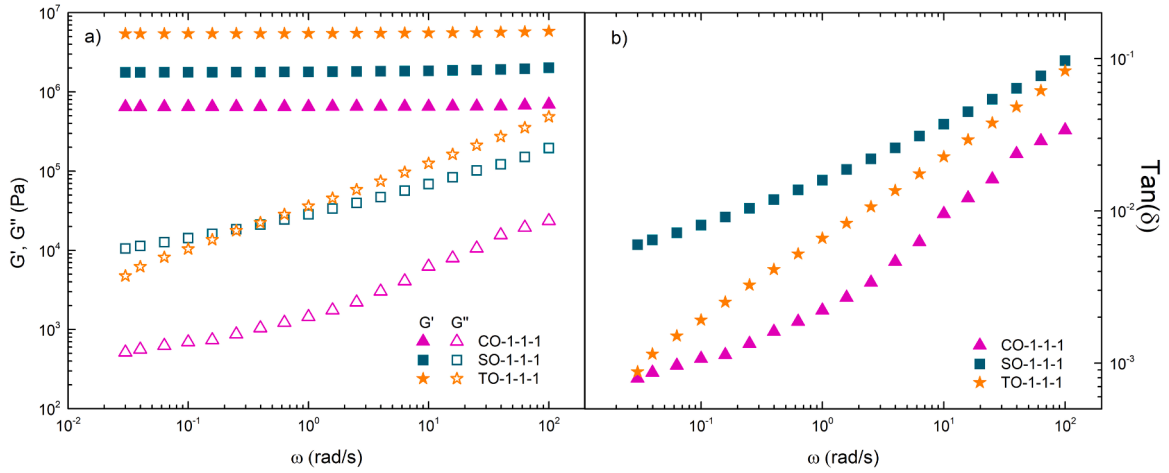

Fig. 9. Frequency dependence of the storage, G', and the loss, G'', moduli (a) and the loss tangent (b) for polymeric thermosets as a function of chemical sites comprising the vegetable oil.

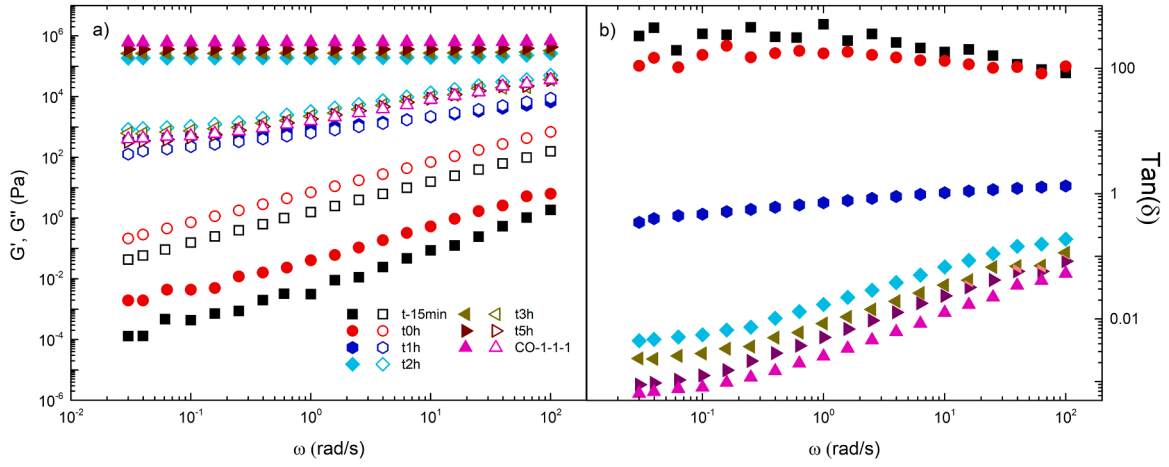

Fig. 10. Monitoring the rheological behaviour of one selected formulation (CO-1–1–1) as a function of curing time (G', filled symbols; G'', empty symbols).

sample CO-1–1–1 in Fig. 10a. G' and G" vs. frequency plots significantly evolve with the curing time. As can be seen, during the raw material mixing phase (t-15 min) and before heating the samples in the oven (t0h), a predominant viscous response was apparent, characterized by G" values higher than those of G' in the whole frequency range studied (Lu et al., 2006). However, as the curing reaction progresses, G'' approaches G 'and eventually gives rise to a crossover. In fact, after 1 h in the oven (t1h curve), G' and G" are almost coincident, roughly indicating the sol-gel transition (Suman and Joshi, 2020). Further, G' increased much more rapidly than G" as a result of the formation of an extended crosslinking network, finally yielding the mechanical response previously described in Fig. 9. This is consistent with the evolution of both the free epoxy rings band in the FTIR spectra and glass transition temperature shown in Fig. 5a and Fig. 5b, respectively, in which a drastic change in the slope of the plots of these parameters is detected after 1 hour of samples curing. Moreover, the loss tangent (see Fig. 10) dramatically decreases from ~200 to ~1 (at 1 rad/s), after 1 h curing, indicating that the sol-gel transition point (tanδ=1) has been approximately reached at this time, and further decreases to around 0.007 for the fully cured system. According to the Winter-Chambon rheological criterion to determine the gel point $G' \propto G'' \propto \omega^n$ (Lu et al., 2006; Nohales et al., 2013), the gelation of these bio-based polyether-polyesters occurs after approximately 1 h upon initiation of the curing process, where the loss tangent is almost independent of frequency and *n* (the frequency dependence of both dynamic functions) is 0.35–0.51(Chuang et al., 2022; Nohales et al., 2013; Wang et al., 2022; Winter and Chambon, 1986). Therefore, a viscoelastic gel was obtained after curing the samples for more than 1 h, when chemical crosslinking among the three functional sites, i.e., hydroxyls or double bonds, anhydride, and epoxy groups, dominates the structure (Lu et al., 2005). In this sense, as can be seen in Fig. 10, the typical rheological behaviour of a crosslinked material was already obtained after 2 h in the oven (t2h sample) (J. Lu, Khot, and Wool, 2005). Hence, the frequency dependency (*n*, $G' \propto \omega^n$) varied with the curing time during the polyether-polyester synthesis process, evolving from the rheological behaviour of a viscoelastic polymer fluid at early stages (t-15 min, $G' \propto \omega^{1.2}$, $G'' \propto \omega^1$) to that of a completely crosslinked solid-like gel ($G' \propto \omega^0$) after curing the samples for 2–5 h (Lu et al., 2006; Zad Bagher Seighalani et al., 2021), which is in line with the results obtained in FTIR and DSC tests (see Fig. 5). A similar trend was previously detailed by some authors, who achieved fully cured materials after shorter periods of the curing process (Indrajati and Dewi, 2017).

Finally, the influence of CO proportion on the rheological properties of these polyether-polyester thermosets is shown in Fig. 11. The molar proportion of double bonds and hydroxyl groups comprising the castor oil was varied concerning anhydride and epoxy groups (see Table 1). By reducing the amount of castor oil used to synthesize the bio-based polyether-polyester (sample CO-0.5–1–1), the number of hydroxyl groups available to react with maleic anhydride decreases, thus remaining unreacted anhydride molecules in the mixture that could further

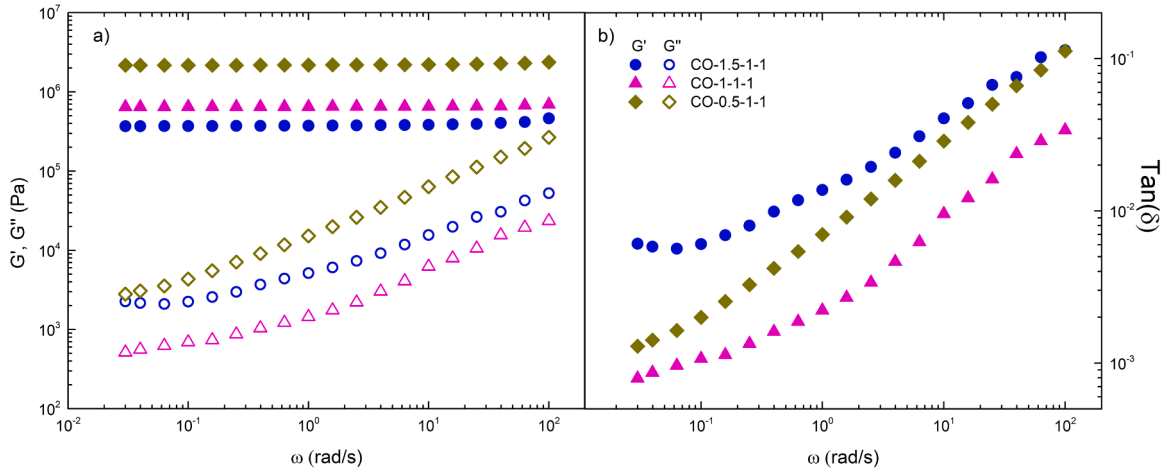

Fig. 11. The storage (G') and the loss (G'') moduli (a) and the loss tangent (b) evolution for CO-based thermosets as a function of the castor oil concentration.

crosslink with epoxy rings. Therefore, the oxirane groups comprising PEGDGE could react with both the −COOH groups of the maleated oil structure and the remaining anhydrides which, in the presence of the catalyst would result in a reinforced network with more crosslinking points (Kolář and Svítilová, 2007). Otherwise, as can be seen in Fig. 11a, an increase in the hydroxyl/anhydride molar ratio in the mixture (sample CO-1.5–1–1) yielded a decrease in both viscoelastic functions. In such cases, two different effects are responsible for the modification in the rheological properties: *i)* the reduced number of crosslinking sites dominating the chemical network characterized by the presence of unreacted hydroxyl groups, and *ii)* the plasticizing effect of castor oil. The modification of the CO proportion in the formulation also resulted in a remarkable variation of the relative elasticity, as revealed by the loss tangent data (Fig. 11b). In this case, more relative elasticity was found for equal molar ratios of the three functional sites dominating the chemical reaction (sample CO-1–1–1), which aligns with the lower values of glass transition temperature previously shown in Table 3.

4. Conclusions

Sustainable polymeric thermosets were obtained by mixing different vegetable oils with maleic anhydride and an epoxy compound, as a result of chemical crosslinking. The chemical reaction between anhydrides and the functional chemical sites in vegetable oils (i.e., double bonds and/or hydroxyl groups) readily activates the chemical structure and promotes the subsequent reaction with epoxy groups, thus producing a permanent rigid three-dimensional network. FTIR, TGA and DSC tests confirmed the chemical crosslinking occurring between the three raw materials. Tung and sunflower oils were observed to undergo the formation of their maleated structures via the scission of double bonds, whereas in castor oil samples, the cleavage of the hydroxyl groups was also evident, as deduced from FTIR tests. On the other hand, the absence of characteristic bands associated with oxirane rings allowed us to verify the reaction between these maleated structures and the epoxy groups, therefore confirming the formation of an extensive crosslinked network. Furthermore, the shifting of the thermal events in polymeric thermosets (i.e., glass transition and melting temperatures for tung and castor, and sunflower oil, respectively) to higher temperatures than their corresponding base oils, suggests an enhancement in the intermolecular forces of the chemical structure leading to chain mobility hindrance. That is typical of materials with a well-defined crosslinked three-dimensional network, which is additionally evidenced by the so-called "rubbery plateau region" of the mechanical spectrum obtained in the rheological tests.

A stronger network dominated by a higher number of crosslinking points was attained as the number of functional sites in the oil fraction rose, thus showing tung oil-based polymers the highest viscoelastic functions. Conversely, castor oil-based polymeric thermosets with less reactive sites exhibited a more flexible structure with enhanced chain mobility and higher relative elastic characteristics. The proportion of vegetable oil in the reacting mixture also produced a remarkable variation in the rheological properties of samples, obtaining a more crosslinked structure when reducing the number of chemical sites in castor oil due to the interaction between unreacted anhydrides molecules in the mixture with epoxy rings.

The progress of the crosslinking reaction was monitored by the evolution of the epoxy peak area in FTIR, the glass transition temperature and the loss tangent with time, obtaining no significant variation of these parameters after 5–6 h, and thus confirming the evolution from a viscoelastic polymer fluid at early stages to that of a completely crosslinked solid-like gel after that period.

Overall, a relatively simple and solvent-free synthesis route is proposed to prepare vegetable oil-based polyether-polyester thermosets with suitable mechanical properties that allow them to be proposed as sustainable alternatives to replace polyurethanes in different applications.

Declaration of Competing Interest

The authors declare that they have no known competing financial interests or personal relationships that could have appeared to influence the work reported in this paper.

Data availability

Data will be made available on request.

Acknowledgements

Funding for open access charge: Universidad de Huelva / CBUA (Spain).

References

Alves, R.S., Maia, D.L.H., de Oliveira, P.H.S., Maia, L.C., Filho, E.G.A., Fernandes, F.A.N., Feitosa, F.X., de Sant'Ana, H.B., 2022. Molecular optimization of castor oil maleate as demulsifier for water-in-crude oil emulsions. Fuel 322, 124204. https://doi.org/10.1016/j.fuel.2022.124204.

Amirova, L.R., Burilov, A.R., Amirova, L.M., Bauer, I., Habicher, W.D., 2016. Kinetics and mechanistic investigation of epoxy – anhydride compositions cured with quaternary phosphonium salts as accelerators. J. Polym. Sci. A Polym. Chem. 54, 1088–1097. https://doi.org/10.1002/pola.27946.

Amos, R.C., Kuska, M., Mesnager, J., Gauthier, M., 2021. Thermally induced maleation of soybean and linseed oils: from benchtop to pilot plant. Ind. Crops Prod. 166, 113504. https://doi.org/10.1016/j.indcrop.2021.113504.
Anastas, P., Eghbali, N., 2010. Green chemistry: principles and practice. Chem. Soc. Rev. 39, 301–312. https://doi.org/10.1039/b918763b.
Balgude, D., Sabnis, A., Ghosh, S.K., 2017. Synthesis and characterization of cardanol based reactive polyamide for epoxy coating application. Prog. Org. Coat. 104, 250–262. https://doi.org/10.1016/j.porgcoat.2016.11.012.
Baumgaertel, M., De Rosa, M.E., Machado, J., Masse, M., Winter, H.H., 1992. The relaxation time spectrum of nearly monodisperse polybutadiene melts. Rheol. Acta 31, 75–82. https://doi.org/10.1007/BF00396469.
Brzeska, J., Piotrowska-Kirschling, A., 2021. A brief introduction to the polyurethanes according to the principles of green chemistry. Processes 9, 1929. https://doi.org/10.3390/pr9111929.
Calligaris, S., Arrighetti, G., Barba, L., Nicoli, M.C., 2008. Phase transition of sunflower oil as affected by the oxidation level. J. Am. Oil Chem. Soc. 85, 591–598. https://doi.org/10.1007/s11746-008-1241-y.
Chen, C., Xu, C., Zhai, J., Zhao, C., Ma, Y., Yang, W., 2023. Low-cost and formaldehyde-free wood adhesive based on water-soluble olefin-maleamic acid copolymers. Ind. Eng. Chem. Res 62, 20547–20555. https://doi.org/10.1021/acs.iecr.3c01968.
Chuang, Y.C., Chang, Y.C., Tsai, M.T., Yang, T.W., Huang, M.T., Wu, S.H., Wang, C., 2022. Electrospinning of Aqueous Solutions of Atactic Poly(N-isopropylacrylamide) with Physical Gelation. Gels 8, 716. https://doi.org/10.3390/gels8110716.
Cucciniello, R., Cespi, D., Riccardi, M., Neri, E., Passarini, F., Pulselli, F.M., 2023. Maleic anhydride from bio-based 1-butanol and furfural: a life cycle assessment at the pilot scale. Green. Chem. 25, 5922. https://doi.org/10.1039/d2gc03707f.
Dayanne, D.L., Alves Filho, E.G., Barros Junior, A.F., Fabiano, F.A., 2018. Kinetics of the production of castor oil maleate through the autocatalyzed thermal reaction and the free radical reaction. Int J. Chem. Kinet. 50, 112–121. https://doi.org/10.1002/kin.21145.
Delli, E., Gkiliopoulos, D., Vouvoudi, E., Bikiaris, D., Chrissafis, K., 2024. Defining the effect of a polymeric compatibilizer on the properties of random polypropylene/glass fibre composites. J. Compos. Sci. 8, 44. https://doi.org/10.3390/jcs8020044.
Devansh, Patil, P., Pinjari, D.V., 2024. Oil-based epoxy and their composites: a sustainable alternative to traditional epoxy. J. Appl. Polym. Sci. 141, e55560. https://doi.org/10.1002/app.55560.
Echeverria-Altuna, O., Ollo, O., Larraza, I., Gabilondo, N., Harismendy, I., Eceiza, A., 2022. Effect of the biobased polyols chemical structure on high performance thermoset polyurethane properties. Polym. (Guildf.) 263, 125515. https://doi.org/10.1016/j.polymer.2022.125515.
Eren, T., Küsefoğlu, S.H., Wool, R., 2003. Polymerization of maleic anhydride-modified plant oils with polyols. J. Appl. Polym. Sci. 90, 197–202. https://doi.org/10.1002/app.12631.
Fahmi, Z., Mudasir, Rohman, A., 2020. Attenuated total reflectance-FTIR spectra combined with multivariate calibration and discrimination analysis for analysis of patchouli oil adulteration. Indones. J. Chem. 20, 1–8. https://doi.org/10.22146/ijc.36955.
Felthouse, T.R., Burnett, J.C., Horrell, B., Mummey, M.J., Kuo, Y., 2000. Maleic Anhydride, Maleic Acid, and Fumaric Acid. in: Kirk-Othmer Encyclopedia of Chemical Technology. John Wiley & Sons. https://doi.org/10.1002/0471238961.1301120506051220.a01.pub2.
Fombuena, V., Petrucci, R., Dominici, F., Jordá-Vilaplana, A., Montanes, N., Torre, L., 2019. Maleinized linseed oil as epoxy resin hardener for composites with high bio content obtained from linen byproducts. Polym. (Basel) 11, 301. https://doi.org/10.3390/polym11020301.
Gomna, A., N'Tsoukpoe, K.E., Le Pierrès, N., Coulibaly, Y., 2020. Thermal stability of a vegetable oil-based thermal fluid at high temperature. Afr. J. Sci., Technol., Innov. Dev. 12, 317–326. https://doi.org/10.1080/20421338.2020.1732080.
Gouveia De Souza, A., Oliveira Santos, J.C., Conceição, M.M., Dantas Silva, M.C., Prasad, S., 2004. A thermoanalytic and kinetic study of sunflower oil. Braz. J. Chem. Eng. 21, 265–273. https://doi.org/10.1590/s0104-66322004000200017.
Hasan, S.O.H., Bircan, I.B., 2022. Preparation of bionanocomposite coatings from tung oil treated with a diamine and a triamine as alternatives for bisphenol A (BPA). Prog. Org. Coat. 168, 106887. https://doi.org/10.1016/j.porgcoat.2022.106887.
Huang, K., Liu, Z., Zhang, J., Li, S., Li, M., Xia, J., Zhou, Y., 2015. A self-crosslinking thermosetting monomer with both epoxy and anhydride groups derived from tung oil fatty acids: synthesis and properties. Eur. Polym. J. 70, 45–54. https://doi.org/10.1016/j.eurpolymj.2015.06.027.
Indrajati, I.N., Dewi, I.R., 2017. Performance of maleated castor oil based plasticizer on rubber: rheology and curing characteristic studies. : IOP Conf. Ser.: Mater. Sci. Eng. IOP Publ., 012001 https://doi.org/10.1088/1757-899X/223/1/012001.
Johns, A., Edwards, K., Inglesby, S., Quirino, R., 2016. Emulsion polymerization of tung oil-based latexes with asolectin as a biorenewable surfactant. Coatings 6, 56. https://doi.org/10.3390/coatings6040056.
Jourdain, A., Obadia, M.M., Duchet-Rumeau, J., Bernard, J., Serghei, A., Tournilhac, F., Pascault, J.P., Drockenmuller, E., 2020. Comparison of poly(ethylene glycol)-based networks obtained by cationic ring opening polymerization of neutral and 1,2,3-triazolium diepoxy monomers. Polym. Chem. 11, 1894–1905. https://doi.org/10.1039/c9py01923e.
Kale, R.D., Jadhav, N.C., Pal, S., 2019. Fabrication of green composites based on rice bran oil and anhydride cross-linkers. Iran. Polym. J. (Engl. Ed.) 28, 471–482. https://doi.org/10.1007/s13726-019-00715-5.
Khundamri, N., Aouf, C., Fulcrand, H., Dubreucq, E., Tanrattanakul, V., 2019. Bio-based flexible epoxy foam synthesized from epoxidized soybean oil and epoxidized mangosteen tannin. Ind. Crops Prod. 128, 556–565. https://doi.org/10.1016/j.indcrop.2018.11.062.
Kolář, F., Svítilová, J., 2007. Kinetics and mechanism of curing epoxy/anhydride systems. Acta Geodyn. Et. Geomater. 4, 85–92.
Kotb, Y., Cagnard, A., Houston, K.R., Khan, S.A., Hsiao, L.C., Velev, O.D., 2022. What makes epoxy-phenolic coatings on metals ubiquitous: surface energetics and molecular adhesion characteristics. J. Colloid Interface Sci. 608, 634–643. https://doi.org/10.1016/J.JCIS.2021.09.091.
Kubota, R., Sugane, K., Shibata, M., 2024. Effect of imine-containing phenolic hardeners with different chain lengths and epoxy functionalities on thermal, mechanical, and healing properties of bio-based epoxy vitrimers. Polym. Bull. 1–18. https://doi.org/10.1007/s00289-024-05327-5.
Liu, N., Wang, H., Ma, B., Xu, B., Qu, L., Fang, D., Yang, Y., 2022. Enhancing cryogenic mechanical properties of epoxy resins toughened by biscitraconimide resin. Compos Sci. Technol. 220, 109252. https://doi.org/10.1016/j.compscitech.2021.109252.
Liu, R., Zhu, G., Li, Z., Liu, X., Chen, Z., Ariyasivam, S., 2015. Cardanol-based oligomers with "hard core, flexible shell" structures: from synthesis to UV curing applications. Green. Chem. 17, 3319–3325. https://doi.org/10.1039/c5gc00366k.
Lu, J., Khot, S., Wool, R.P., 2005. New sheet molding compound resins from soybean oil. I. Synthesis and characterization. Polym. (Guildf.) 46, 71–80. https://doi.org/10.1016/j.polymer.2004.10.060.
Lu, L., Liu, X., Tong, Z., 2006. Critical exponents for sol-gel transition in aqueous alginate solutions induced by cupric cations. Carbohydr. Polym. 65, 544–551. https://doi.org/10.1016/j.carbpol.2006.02.010.
Mattar, N., Anda, A.R., De, Vahabi, H., Renard, E., De Anda, A.R., Vahabi, H., Renard, E., Langlois, V., 2020. Resorcinol-based epoxy resins hardened with limonene and eugenol derivatives: from the synthesis of renewable diamines to the mechanical properties of biobased thermosets. ACS Sustain Chem. Eng. 8, 13064–13075. https://doi.org/10.1021/acssuschemeng.0c04780.
Michel, M., Ferrier, E., 2020. Effect of curing temperature conditions on glass transition temperature values of epoxy polymer used for wet lay-up applications. Constr. Build. Mater. 231, 117206. https://doi.org/10.1016/j.conbuildmat.2019.117206.
Morsch, S., Wand, C.R., Gibbon, S., Irwin, M., Siperstein, F., Lyon, S., 2023. The effect of cross-linker structure on interfacial interactions, polymer dynamics and network composition in an epoxy-amine resin. Appl. Surf. Sci. 609, 155380. https://doi.org/10.1016/j.apsusc.2022.155380.
Nabipour, H., Rohani, S., Hu, Y., 2023. A bio-based epoxy resin derived from syringaldehyde with excellent mechanical properties, flame retardant and high glass transition temperature. Polym. Degrad. Stab. 214, 110410. https://doi.org/10.1016/j.polymdegradstab.2023.110410.
Nohales, A., López, D., Culebras, M., Gómez, C.M., 2013. Rheological study of gel phenomena during epoxide network formation in the presence of sepiolite. Polym. Int 62, 397–405. https://doi.org/10.1002/pi.4321.
Omonov, T.S., Patel, V., Curtis, J.M., 2019. The development of epoxidized hemp oil prepolymers for the preparation of thermoset networks. J. Am. Oil Chem. Soc. 96, 1389–1403. https://doi.org/10.1002/aocs.12290.
Panhwar, T., Mahesar, S.A., Kandhro, A.A., Sheerazi, S.T.H., Kori, A.H., Laghari, Z.H., Memon, J.-R., 2019. Physicochemical composition and FTIR characterization of castor seed oil. Ukr. Food J. 8, 778–787. https://doi.org/10.24263/2304-974x-2019-8-4-9.
Parada Hernandez, N.L., Bahú, J.O., Schiavon, M.I.R.B., Bonon, A.J., Benites, C.I., Jardini, A.L., Maciel Filho, R., Wolf Maciel, M.R.W., 2019. Epoxidized castor oil – citric acid) copolyester as a candidate polymer for biomedical applications. J. Polym. Res. 26, 1–10. https://doi.org/10.1007/s10965-019-1814-5.
Poletto, M., 2019. Maleated soybean oil as coupling agent in recycled polypropylene/wood flour composites: mechanical, thermal, and morphological properties. J. Thermoplast. Compos. Mater. 32, 1056–1067. https://doi.org/10.1177/0892705718785707.
Raghavan, S.R., Chen, L.A., McDowell, C., Khan, S.A., Hwang, R., White, S., 1996. Rheological study of crosslinking and gelation in chlorobutyl elastomer systems. Polym. (Guildf.) 37, 5869–5875.
Rohman, A., Che Man, Y.B., 2012. Quantification and classification of corn and sunflower oils as adulterants in olive oil using chemometrics and FTIR spectra. Sci. World J. 2012, 250795. https://doi.org/10.1100/2012/250795.
Rosu, D., Mustata, F., Tudorachi, N., Musteata, V.E., Rosu, L., Varganici, C.D., 2015. Novel bio-based flexible epoxy resin from diglycidyl ether of bisphenol A cured with castor oil maleate. RSC Adv. 5, 45679–45687. https://doi.org/10.1039/c5ra05610a.
Saeedi, I.A., Andritsch, T., Vaughan, A.S., 2019. On the dielectric behavior of amine and anhydride cured epoxy resins modified using multi-terminal epoxy functional network modifier. Polym. (Basel) 11, 1271. https://doi.org/10.3390/polym11081271.
Şahin, Y.M., Çayli, G., Çavuşoğlu, J., Tekay, E., Şen, S., 2016. Cross-linkable epoxidized maleinated castor oil: a renewable resin alternative to unsaturated polyesters. Int J. Polym. Sci. 2016, 5781035. https://doi.org/10.1155/2016/5781035.
Sain, S., Åkesson, D., Skrifvars, M., 2020. Synthesis and properties of thermosets from tung oil and furfuryl methacrylate. Polym. (Basel) 12, 1–16. https://doi.org/10.3390/polym12020258.
Schönemann, A., Edwards, H.G.M., 2011. Raman and FTIR microspectroscopic study of the alteration of Chinese tung oil and related drying oils during ageing. Anal. Bioanal. Chem. 400, 1173–1180. https://doi.org/10.1007/s00216-011-4855-0.
Sharma, V., Kundu, P.P., 2006. Addition polymers from natural oils—a review. Prog. Polym. Sci. 31, 983–1008. https://doi.org/10.1016/J.PROGPOLYMSCI.2006.09.003.
Silva, R.S., Maia, D.L.H., Fernandes, F.A.N., 2021. Production of tung oil epoxy resin using low frequency high power ultrasound. Ultrason Sonochem. 79, 105765. https://doi.org/10.1016/j.ultsonch.2021.105765.

Subramanian, K., 2019. A comprehensive study on thermal degdradation of selective edible vegetable oils by simultaneous thermogravimetric and differential thermal analyses. J. Pharm. Sci. Res. 11, 3201–3209.
Suman, K., Joshi, Y.M., 2020. Kinetic model for a sol-gel transition: application of the modified Bailey criterion. Rheol. Acta 59, 745–753. https://doi.org/10.1007/s00397-020-01237-1.
Tamási, K., Marossy, K., 2022. Combined thermal analysis of plant oils. J. Therm. Anal. Calor. 147, 2047–2054. https://doi.org/10.1007/s10973-020-10470-y.
Tang, J., Zhang, J., Lu, J., Huang, J., Zhang, F., Hu, Y., Liu, C., An, R., Miao, H., Chen, Y., Huang, T., Zhou, Y., 2020. Preparation and properties of plant-oil-based epoxy acrylate-like resins for UV-curable coatings. Polym. (Basel) 12, 2165. https://doi.org/10.3390/polym12092165.
Teng, X., Xu, H., Song, W., Shi, J., Xin, J., Hiscox, W.C., Zhang, J., 2017. Preparation and properties of hydrogels based on PEGylated lignosulfonate amine. ACS Omega 2, 251–259. https://doi.org/10.1021/acsomega.6b00296.
Thakur, V.K., Thakur, M.K., Voicu, S.I., 2018. Polymer gels: perspectives and applications. : Gels Horiz.: Sci. Smart Mater. 2018.
Tran, P., Seybold, K., Graiver, D., Narayan, R., 2005. Free Radic. Maleation Soybean Oil via a Single-Step Process 82, 189–194. https://doi.org/10.1007/s11746-005-5171-7.
Tudorachi, N., Mustata, F., 2020. Curing and thermal degradation of diglycidyl ether of bisphenol A epoxy resin crosslinked with natural hydroxy acids as environmentally friendly hardeners. Arab. J. Chem. 13, 671–682. https://doi.org/10.1016/j.arabjc.2017.07.008.
Wang, C., Hashimoto, T., Chuang, Y.C., Tanaka, K., Chang, Y.P., Yang, T.W., Huang, M. T., 2022. Physical gelation of aqueous solutions of atactic poly(N-isopropylacrylamide). Macromolecules 55, 9152–9167. https://doi.org/10.1021/acs.macromol.1c02476.
Wazarkar, K., Sabnis, A., 2018. Cardanol based anhydride curing agent for epoxy coatings. Prog. Org. Coat. 118, 9–21. https://doi.org/10.1016/j.porgcoat.2018.01.018.
Winter, H.H., Chambon, F., 1986. Analysis of linear viscoelasticity of a crosslinking polymer at the gel point. J. Rheol. 30, 367–382. https://doi.org/10.1122/1.549853.
Wu, Y., Hu, Y., Lin, H., Zhang, X., 2024. An anhydride-cured degradable epoxy insulating material exhibiting recyclability, reusability, and excellent electrical performance. Green. Chem. 26, 2258. https://doi.org/10.1039/d3gc04580c.
Xiao, L., Liu, Z., Li, N., Li, S., Fu, P., Wang, Y., Huang, J., Chen, J., Nie, X., 2020. A hyperbranched polymer from tung oil for the modification of epoxy thermoset with simultaneous improvement in toughness and strength. N. J. Chem. 44, 16856–16863. https://doi.org/10.1039/c9nj06373k.
Yang, G., Rohde, B.J., Tesefay, H., Robertson, M.L., 2016. Biorenewable epoxy resins derived from plant-based phenolic acids. ACS Sustain Chem. Eng. 4, 6524–6533. https://doi.org/10.1021/acssuschemeng.6b01343.
Yi, Y., Yao, J., Xu, W., Wang, L.M., Wang, H.X., 2019. Investigation on the quality diversity and quality-FTIR characteristic relationship of sunflower seed oils. RSC Adv. 9, 27347–27360. https://doi.org/10.1039/c9ra04848k.
Zad Bagher Seighalani, F., McMahon, D.J., Sharma, P., 2021. Determination of critical gel-sol transition point of Highly Concentrated Micellar Casein Concentrate using multiple waveform rheological technique. Food Hydrocoll. 120, 106886. https://doi.org/10.1016/j.foodhyd.2021.106886.
Zhang, J., Shang, Q., Hu, Y., Zhang, F., Huang, J., Lu, J., Cheng, J., Liu, C., Hu, L., Miao, H., Chen, Y., Huang, T., Zhou, Y., 2020. High-biobased-content UV-curable oligomers derived from tung oil and citric acid: Microwave-assisted synthesis and properties. Eur. Polym. J. 140, 109997. https://doi.org/10.1016/j.eurpolymj.2020.109997.
Zhen, X., Cui, X., Al-Haimi, A.A.N.M., Wang, X., Liang, H., Xu, Z., Wang, Z., 2024. Fully bio-based epoxy resins from lignin and epoxidized soybean oil: rigid-flexible, tunable properties and high lignin content. Int J. Biol. Macromol. 254, 127760. https://doi.org/10.1016/j.ijbiomac.2023.127760.